

Supersolid Phase of Cold Fermionic Polar Molecules in 2D Optical Lattices

Liang He and Walter Hofstetter

Institut für Theoretische Physik, Johann Wolfgang Goethe-Universität, 60438 Frankfurt/Main, Germany

We study a system of ultra-cold fermionic polar molecules in a two-dimensional square lattice interacting via both the long-ranged dipole-dipole interaction and a short-ranged on-site attractive interaction. Singlet superfluid, charge density wave, and supersolid phases are found to exist in the system. We map out the zero temperature phase diagram and find that the supersolid phase is considerably stabilized by the dipole-dipole interaction and thus can exist over a large region of filling factors. We study the melting of the supersolid phase with increasing temperature, map out a finite temperature phase diagram of the system at fixed filling, and determine the parameter region where the supersolid phase can possibly be observed in experiments.

PACS numbers: 03.75.Ss, 67.85.-d, 05.30.Fk

I. INTRODUCTION

Ultracold atom physics has undergone spectacular development in the last two decades. During the last years, after the first theoretical proposal to simulate the Bose-Hubbard model with ultracold bosons in an optical lattice [1] and its successful experimental realization [2], considerable theoretical and experimental progress has been made on degenerate quantum gases in optical lattices [3]. One major common goal shared by these efforts is to simulate typical systems or minimal models of condensed matter physics, e.g. the Hubbard model, using ultracold atoms confined in optical lattices [4, 5]. It is expected that these investigations can give key insights into unresolved open questions in condensed matter physics, e.g. the mechanism of high- T_c superconductivity. Usually, interactions in cold gases are isotropic and short ranged. Naturally one can ask the question which type of new physics would arise in these systems if the atoms have additional long-range anisotropic interactions.

As a matter of fact, a wealth of interesting physics has already been revealed by theoretical and experimental investigations of ultracold dipolar Bose gases both in harmonic traps [6–14] and optical lattices [15–18]. In contrast to dipolar Bose gases, due to the Pauli exclusion principle, dipolar effects in fermionic systems can manifest themselves only if the dipolar interaction energy is at least of the order of the Fermi energy. Although there have been already some theoretical investigations on these systems [19–23], this condition could hardly be reached experimentally until the recent successful realization of a degenerate quantum gas of fermionic $^{40}\text{K}^{87}\text{Rb}$ polar molecules [24]. With this achievement, the door towards exploring the many-body physics originating from dipole-dipole interactions in fermionic systems has been opened, which has already lead to a number of theoretical investigations on these systems [25–43]. Motivated by experimental progress on ultracold polar molecules, here we investigate the low temperature quantum phases of a system of cold polar fermions loaded into a 2D square optical lattice.

The rest part of this paper is organized as follows. In

Sec. II, we introduce the system and the model studied here. In Sec. III, we describe the theoretical approach used in our investigation. In Sec. IV, the main section of this paper, we present a detailed discussion of the quantum phases at both zero and finite temperature. Finally, we conclude in Sec. V.

II. SYSTEM AND MODEL

Motivated by ongoing experiments, we focus our investigations on possible setups based on $^{40}\text{K}^{87}\text{Rb}$ molecules which have a permanent electric dipole moment of 0.57 Debye (D), where $1\text{D} = 3.336 \times 10^{-30}\text{C} \cdot \text{m}$. However the effective dipole moment in the laboratory frame is zero in the absence of an external electric field. When an external electric field is applied the molecules align with the field and have an induced dipole moment d which increases with the strength of the external field. Currently, the experimentally accessible range of d is $[0, 0.22 D]$ [44]. In this work we assume the external electric field is oriented perpendicular to the optical lattice plane.

Loading the molecules into an optical lattice, the physics of this system for sufficiently low filling can be captured by an extended Hubbard model within the lowest band approximation,

$$H = -t \sum_{\langle i,j \rangle, \sigma} c_{i\sigma}^\dagger c_{j\sigma} + U \sum_i n_{i\uparrow} n_{i\downarrow} + \frac{c_d}{2} \sum_{i \neq j; \sigma \sigma'} \frac{n_{i\sigma} n_{j\sigma'}}{|\mathbf{R}_i - \mathbf{R}_j|^3} - \mu \sum_{i\sigma} n_{i\sigma}. \quad (1)$$

Here, $\langle i, j \rangle$ denotes nearest-neighbour sites, $c_{i\sigma}^\dagger$ ($c_{i\sigma}$) is the creation (annihilation) operator of a fermionic molecule with spin σ on site i in the Wannier representation, and $n_{i\sigma} = c_{i\sigma}^\dagger c_{i\sigma}$ is the particle number operator. The first term in Eq. (1) describes the kinetic energy with t being the hopping amplitude; the second term represents the onsite interaction U between molecules with opposite spin; the third term originates from the long-range dipole-dipole interactions, where $c_d = d^2/(4\pi\epsilon_0 a^3)$ characterizes the dipole-dipole interaction strength with a

and ε_0 being the lattice constant and the vacuum permittivity respectively, and \mathbf{R}_i is the dimensionless position vector of lattice site i ; finally, in the last term μ denotes the chemical potential.

In our calculations we assume a 2D optical lattice created by laser beams with wavelength $\lambda = 1064\text{nm}$ as used in the experimental setup of Ref. [44]. We consider the following parameters: the height of the lattice potential in the direction perpendicular to the lattice plane V_z^{lat} and parallel to the plane V_{\perp}^{lat} are chosen as $V_{\perp}^{\text{lat}} = 10E_R$, $V_z^{\text{lat}} = 10V_{\perp}^{\text{lat}}$, where $E_R = \hbar^2/(2m\lambda^2)$ is the recoil energy, m is the mass of molecule and \hbar is Planck's constant. Under these conditions, the dipolar interaction strength is in the range $[0, 0.03E_R]$, and the hopping amplitude is approximately $0.2E_R$. Therefore the ratio between the dipolar interaction strength and the hopping amplitude c_d/t is approximately in the range $[0, 0.15]$, which we assume in our calculations.

A good estimate of the strength of the onsite interaction U requires a detailed study of all types of short-range interactions between the polar molecules, which is beyond the scope of this work. Since the main aim of this work is to investigate the possibility of observing a supersolid phase of polar molecules, we assume that the onsite interaction is attractive, i.e., $U < 0$. Moreover, we notice that since large attractive on-site interactions will make the system unstable, the region of $|U|$ investigated in this work is restricted to $[t, 8t]$.

On the route towards observing the supersolid phase in experiments, the temperature plays a dominant role. In current experiments with polar molecules in a harmonic trap, the lowest temperature which can be reached is of the order of the Fermi temperature T_F [44]. Also, when the lattice potential is ramped up, generally, the molecules will be heated in this process, which results in even higher temperatures. In the following, the system is studied at both zero and finite temperatures, and the temperature region where a supersolid phase can be possibly observed is determined.

III. METHOD

Before discussing our results in detail, we give a brief description of our theoretical approach. In polar molecule systems, we have to consider not only the on-site attraction of the molecules but also the inter-site repulsion due to the dipolar interaction. For treating the on-site interactions, the Dynamical Mean-Field Theory (DMFT) [47] is well suited since it is non-perturbative, captures the local quantum fluctuation exactly, and gives exact results in the infinite-dimensional limit. For long-ranged interactions in fermionic system, on the other hand, there are, to our knowledge, up to now only few efficient ways to treat them, although DMFT has already been generalized to the so called cellular DMFT in order to treat short-range inter-site interactions [48].

We include long-range interactions as follows. First

we notice that in the high-dimensional limit inter-site interactions only contribute on the Hartree level [49]. In other words, the Hartree term of the inter-site interaction will dominate as the spatial dimension of the system increases. This motivates us to keep only the Hartree contribution of the inter-site interaction in the Hamiltonian as an approximation to the original Hamiltonian (1), i.e.

$$\frac{c_d}{2} \sum_{i \neq j; \sigma \sigma'} \frac{n_{i\sigma} n_{j\sigma'}}{|\mathbf{R}_i - \mathbf{R}_j|^3} \quad (2)$$

$$\simeq \sum_{i \neq j; \sigma \sigma'} c_d \frac{1}{|\mathbf{R}_i - \mathbf{R}_j|^3} \langle n_{j\sigma} \rangle (n_{i\sigma'} - \frac{1}{2} \langle n_{i\sigma'} \rangle). \quad (3)$$

Our DMFT Hamiltonian therefore takes the form

$$H = -t \sum_{\langle i, j \rangle, \sigma} c_{i\sigma}^\dagger c_{j\sigma} + U \sum_i n_{i\uparrow} n_{i\downarrow} + \sum_{i\sigma} (\tilde{V}_i - \mu) n_{i\sigma} \quad (4)$$

where

$$\tilde{V}_i = \sum_{j (i \neq j), \sigma} c_d \frac{1}{|\mathbf{R}_i - \mathbf{R}_j|^3} \langle n_{j\sigma} \rangle \quad (5)$$

and we have rescaled the chemical potential μ in (4) according to the trivial constant term in (3).

We investigate this system using real-space DMFT (R-DMFT)[45, 46], which is an extension of DMFT to a position-dependent self-energy and fully captures the inhomogeneity of the system. Within DMFT/R-DMFT, the physics on each lattice site is determined from a local effective action which can be captured by an effective Anderson impurity model [47]. In this work, we use Exact Diagonalization (ED) [50, 51] of the Anderson impurity Hamiltonian to solve the local action. Details of the R-DMFT method can be found in previous works [45, 46].

Within each R-DMFT iteration, the Hartree contributions \tilde{V}_i are calculated and the Hamiltonian (4) is updated according to the new values \tilde{V}_i . This modified R-DMFT iteration is repeated until a convergent solution is obtained.

IV. RESULTS

A. Zero temperature

1. Phase diagram

At zero temperature, the main properties of the system are summarized in the phase diagram in Fig. 1, which shows the phase boundary between the supersolid (SS) phase and the homogeneous singlet superfluid phase (HSF) at different onsite interaction strengths U in terms of the filling factor $\rho \equiv \sum_{i\sigma} \langle n_{i\sigma} \rangle / N$ and the dipolar interaction strength c_d , where N is the number of lattice sites. This phase diagram is based on calculations for a 12×12 square lattice. We will denote the phase boundary

between the supersolid (SS) phase and the homogeneous singlet superfluid phase the *SS-HSF boundary* in the following.

Along the vertical line at half filling ($\rho = 1$) in Fig. 1, irrespective of the strengths of on-site and inter-site interactions, the system is always in an incompressible charge density wave (CDW) phase, which is characterized both by vanishing compressibility $\partial\rho/\partial\mu = 0$ and a finite density modulation in real space. More specifically, the density distribution over the lattice has a checkerboard (CB) structure, which is characterized by $\rho_{\mathbf{Q}} \equiv \sum_j e^{i\mathbf{Q}\cdot\mathbf{R}_j} \rho_j / N$ with $\rho_j \equiv \sum_{\sigma} \langle n_{j\sigma} \rangle$ and $\mathbf{Q} = (\pi, \pi)$. In our calculations, we choose $\rho_{\mathbf{Q}}$ as the CDW order parameter and we will denote this incompressible CDW phase as ‘‘CB solid’’.

Away from half filling but still in the region bounded by the SS-HSF boundary and the vertical line of half filling, a supersolid phase is obtained by doping the CB solid with either particles or vacancies, which is characterized by the coexistence of the singlet pairing order parameter $\Delta_i \equiv \langle c_{i\downarrow} c_{i\uparrow} \rangle$ and the CDW order $\rho_{\mathbf{Q}}$. As we can see from Fig. 1, at fixed on-site interaction strength U , the filling region in which the system remains supersolid increases with the strength of the dipolar interaction. This can be understood by the following simple argument. We notice that near the SS-HSF boundary the dominant contribution to the inter-site interaction energy between two nearest neighbor sites i, j is positive and approximately proportional to $c_d \rho_i \rho_j \sim c_d (\rho^2 - (\rho_i - \rho_j)^2/4)$, therefore a larger c_d will make the system more likely to favor a modulated density distribution since it can lower the intersite interaction energy in this way. On the other hand, at fixed dipolar interaction strength c_d , we can see from Fig. 1 that a larger on-site attraction strength $|U|$ corresponds to a larger supersolid filling factor region. This can be understood by a similar argument as above. We notice that near the SS-HSF boundary the total on-site interaction energy of two neighboring sites is approximately proportional to $-|U|(\rho_i^2 + \rho_j^2) \sim -|U|(\rho^2 + (\rho_i - \rho_j)^2/4)$, one can thus easily see that for large $|U|$ the system will favor a large density imbalance between neighboring sites which results in a modulated density distribution.

Concerning the proposed experimental setup with $^{40}\text{K}^{87}\text{Rb}$ molecules in an optical lattice, according to the discussions above, the supersolid phase will be observed more easily in an interaction region with relatively large dipolar interaction and onsite attraction, since this will stabilize the supersolid in a large filling factor region, e.g. in the range $\rho \in (1.0, 1.4)$ for interaction strengths $c_d = 0.1t$ and $U = -8t$.

On the right-hand side of the SS-HSF boundary, the system is in a homogeneous singlet superfluid phase which is characterized by a uniform distribution of both the density ρ_i and the singlet pairing order parameter Δ_i .

We note that in the classical limit of zero hopping, the long-range interacting model exhibits a devil’s staircase of various solid phases [52]. Therefore, for much larger c_d , which far exceeds the region investigated in this work, one

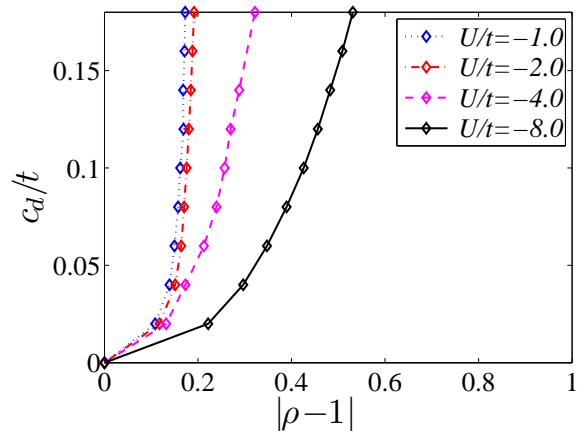


Figure 1: (Color online). Phase diagram of the system with respect to the filling per lattice site ρ and the strength of dipolar interaction c_d , obtained from calculations on a 12×12 square lattice. Different curves indicate the phase boundaries between supersolid (SS) and homogeneous singlet superfluid (HSF) at different onsite interaction strengths U . On the left-hand side of each curve the system is in the SS phase (except exactly at half filling ($\rho = 1.0$)) while the right-hand side region indicates the homogeneous singlet superconducting phase. From left to right, different curves correspond to $U/t = -1.0, -2.0, -4.0,$ and -8.0 respectively.

would expect to find other types of incompressible CDW phases rather than CB solid and possibly new SS phases similar to those found for dipolar Bose gases in optical lattices [17, 18]. A detailed investigation of this ‘‘devil’s staircase’’ in the quantum case is beyond the scope of this current work.

2. Density and singlet pairing order parameter distribution

Recently, there has been considerable progress in single-site addressability in optical lattices using electron and optical microscopy which allows for a direct, *in situ*, experimental observation of particle positions and density-density correlations of the system [53–56]. In Fig. 2 we show three sets of snapshots of the density and pairing order parameter distributions of the system for the different phases discussed previously. We observe that the system develops the (π, π) density modulation in both the CB solid and SS phase. Moreover in the SS phase the amplitude of the pairing order parameter Δ_i also has a similar spatial checkerboard modulation. In the HSF phase both the density and the pairing order parameter are constant over the lattice. We remark here that although the distribution of density and pairing order parameter is obtained in the absence of the external trapping potential, the typical feature of these phases can nevertheless be observed at the center of a shallow harmonic trap where a local density approximation is valid.

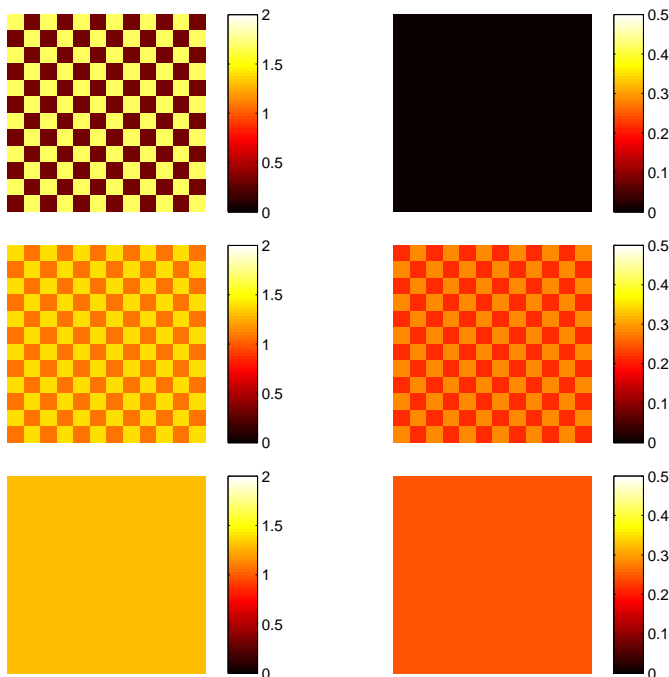


Figure 2: (Color online). Zero temperature density ρ_i (left panel) and singlet pairing order parameter Δ_i (right panel) distribution of the system ($U = -4.0t$, $c_d = 0.1t$). In descending order, the filling factor has the values $\rho = 1.0$, 1.28 , and 1.46 respectively, corresponding to the checkerboard solid, supersolid, and homogeneous singlet superfluid.

B. Finite temperature

In this subsection we investigate finite temperature effects and calculate the critical temperature of the supersolid which could be useful as a guide for future experiments.

First, we study the melting process of the supersolid to a normal phase with increasing T at fixed filling. Fig. 3 shows the temperature dependence of the CDW order parameter $\rho_{\mathbf{Q}}$ and the average value of singlet pairing order parameter $\Delta \equiv \sum_j \Delta_j / N$, which is used to characterize the superfluidity of the system, for $U = -4.0t$, $c_d = 0.1t$ and filling factor $\rho = 1.2$. The SS melts into a normal phase via two successive transitions. First, it melts into a phase with zero pairing order parameter Δ_i but finite $\rho_{\mathbf{Q}}$ at the temperature $T \simeq 0.2t/k_B$, where k_B is the Boltzmann constant. We will denote this phase CDW in the following discussion. One interesting behavior to be noted in this step of the melting process is that as T increases the CDW order parameter keeps growing to a maximum until the pairing order Δ decreases to zero, which is quite different from the melting processes of bosonic supersolids investigated in Ref. [17, 18]. The physical reason for this behavior is the competition between pairing and CDW order in the system. Similar phenomena have already been observed in previous studies of condensed matter systems, see e.g. Ref. [57]. To

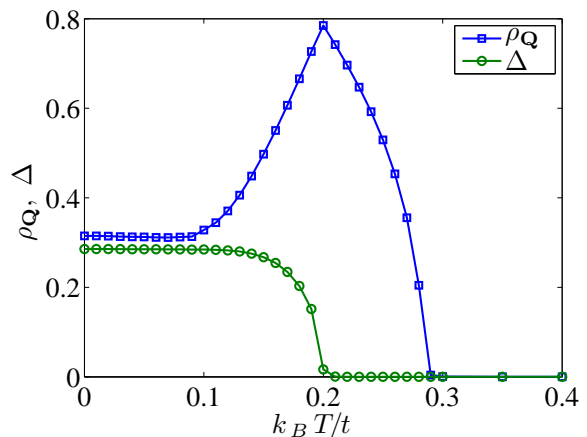


Figure 3: (Color online). Melting of the supersolid with increasing temperature ($U = -4.0t$, $c_d = 0.1t$, $\rho = 1.2$). Squares and circles correspond to the temperature dependence of the CDW order $\rho_{\mathbf{Q}}$ and the average value of the pairing order parameters Δ , which is used to characterize the superfluidity of the system, respectively.

clarify this point, in the vicinity of the phase transition where both order parameters are small, we calculate the Ginzburg-Landau (GL) free energy of the system up to the 4th order:

$$F = A_{\Delta}|\Delta|^2 + A_{\rho}|\rho_{\mathbf{Q}}|^2 + B_{\Delta}|\Delta|^4 + B_{\rho}|\rho_{\mathbf{Q}}|^4 + C_{\Delta\rho}|\Delta|^2|\rho_{\mathbf{Q}}|^2. \quad (6)$$

Here $\{A_{\Delta}, B_{\Delta}, A_{\rho}, B_{\rho}, C_{\Delta\rho}\}$ are the GL coefficients where a positive $C_{\Delta\rho}$ indicates competition between the two types of order. A detailed calculation (see appendix A) shows that $C_{\Delta\rho}$ is indeed positive, thus justifying the physical picture given above. Upon further increase of the temperature T , the CDW order parameter $\rho_{\mathbf{Q}}$ decreases to zero at $T \simeq 0.29t/k_B$.

Moreover, we map out a phase diagram of the system with respect to temperature T and the dipolar interaction strength c_d for onsite attraction $U = -4.0t$ at fixed filling $\rho = 1.2$, see Fig. 4. When we lower the system temperature, for weak dipolar interaction ($c_d < 0.05t$) we observe a transition from the normal to the HSF phase. While in a very narrow region $0.05t < c_d < 0.07t$, we observe first a transition between a normal phase (white region) and a CDW phase (yellow region), then a transition into the SS phase (green region), and finally a transition into the HSF (blue region) which is due to the competition between CDW order and pairing as discussed above. At larger dipolar interaction strength ($c_d > 0.07t$), we observe first a transition between the normal phase and the CDW phase, then a transition into the supersolid. As can be seen from Fig. 4, in order to observe the supersolid for these parameters, c_d should be larger than $0.05t$, with a maximum critical temperature of about $0.22t/k_B$ which is approximately $0.1T_F$. In comparison to the lowest temperatures reached in current experiments with polar molecules in a harmonic trap, which are of order T_F

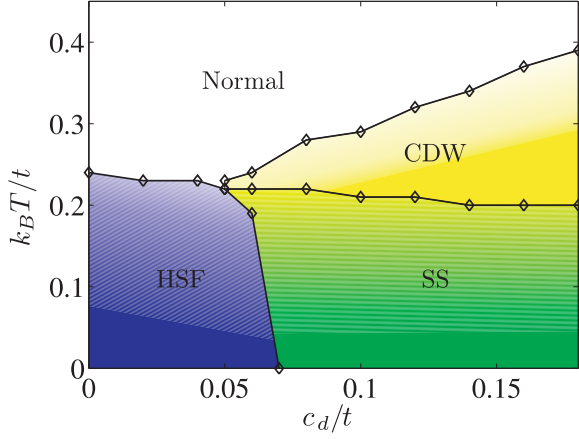


Figure 4: (Color online). Finite temperature phase diagram for $U = -4.0t$ and filling $\rho = 1.2$ obtained from calculations on a 12×12 square lattice. See the text for details.

[44], this means that the temperature still has to be lowered by one order of magnitude in order to observe the supersolid. But given major theoretical and experimental efforts in lowering the temperature of cold atoms and molecules in optical lattices [58–62], we expect this supersolid phase will be accessible experimentally in the near future.

V. CONCLUSION

In conclusion, we have shown that when fermionic polar molecules are loaded into a 2D square lattice, this system will exhibit a supersolid phase which can be observed in an experimental setup based on $^{40}\text{K}^{87}\text{Rb}$ molecules provided the lowest temperature of current experiments can be lowered by one order of magnitude.

Acknowledgments

We acknowledge useful discussions with E. Altman, I. Bloch and E. Demler. L. He thanks I. Titvinidze and A. Privitera for many helpful discussions and technical support at the beginning of this work. This work was supported by the German Science Foundation DFG via the DIP project BL 574/10-1.

Appendix A: Calculation of GL coefficients

In this appendix, we give the detailed calculation of the GL coefficients from the microscopic Hamiltonian (1) in

the Bloch representation, i.e.,

$$H = \sum_{\mathbf{k}\sigma} (\varepsilon(\mathbf{k}) - \mu) c_{\mathbf{k}\sigma}^\dagger c_{\mathbf{k}\sigma} + \frac{U}{N} \sum_{\mathbf{k}_1 \mathbf{k}_2 \mathbf{q}} c_{\mathbf{k}_1 + \mathbf{q}\uparrow}^\dagger c_{\mathbf{k}_2 - \mathbf{q}\downarrow}^\dagger c_{\mathbf{k}_2\downarrow} c_{\mathbf{k}_1\uparrow} + \frac{1}{2} \sum_{\mathbf{q}} \frac{V(\mathbf{q})}{N} \hat{\rho}_{\mathbf{q}} \hat{\rho}_{-\mathbf{q}}, \quad (\text{A1})$$

where

$$\hat{\rho}_{\mathbf{q}} = \sum_{\mathbf{k}\sigma} c_{\mathbf{k}+\mathbf{q},\sigma}^\dagger c_{\mathbf{k},\sigma}, \quad (\text{A2})$$

$$V(\mathbf{q}) = \sum_{|\mathbf{R}_j| \neq 0} e^{-i\frac{2\pi}{N}\mathbf{q}\cdot\mathbf{R}_j} \frac{c_d}{|\mathbf{R}_j|^3} \quad (\text{A3})$$

and $\varepsilon(\mathbf{k})$ is Fourier transformation of the hopping matrix. The partition function of the system can be written in the path-integral form of $\mathcal{Z} = \int \mathcal{D}[\bar{c}_{k\sigma}, c_{k\sigma}] e^{-S[\bar{c}_{k\sigma}, c_{k\sigma}]}$ where the action of the system is

$$\begin{aligned} S[\bar{c}_{k\sigma}, c_{k\sigma}] &= \sum_k \sum_{\sigma} (-i\omega_n + \varepsilon(\mathbf{k}) - \mu) \bar{c}_{k\sigma} c_{k\sigma} \\ &+ \frac{U}{\beta N} \sum_{k_1 k_2 q} \bar{c}_{k_1 + q\uparrow} \bar{c}_{k_2 - q\downarrow} c_{k_2\downarrow} c_{k_1\uparrow} \\ &+ \frac{1}{2} \frac{1}{\beta N} \sum_q V(\mathbf{q}) \sum_{kk'\sigma\sigma'} \bar{c}_{k+q,\sigma} c_{k,\sigma} \bar{c}_{k'-q,\sigma'} c_{k',\sigma'} \end{aligned} \quad (\text{A4})$$

where $\omega_n = (2n + 1)\pi/\beta$ is fermionic Matsubara frequency with $\beta = 1/(k_B T)$ being the inverse temperature and q, k are three-momentum comprising a vectorial momentum in 2-dimensional space and a fermionic Matsubara frequency. Now by performing two Hubbard-Stratonovich transformations

$$\begin{aligned} &\exp\left[\frac{|U|}{\beta N} \sum_{k_1 k_2 q} \bar{c}_{k_1 + q\uparrow} \bar{c}_{k_2 - q\downarrow} c_{k_2\downarrow} c_{k_1\uparrow}\right] \\ &= \int \mathcal{D}(\chi, \bar{\chi}) \exp\left\{-\sum_q \frac{\beta N}{|U|} |\chi_q|^2 + \bar{\chi}_q \left(\sum_k c_{k\downarrow} c_{q-k\uparrow}\right) + \left(\sum_k \bar{c}_{q-k\uparrow} \bar{c}_{k\downarrow}\right) \chi_q\right\}, \quad (\text{A5}) \\ &\exp\left[-\sum_q \frac{1}{2} \frac{V(\mathbf{q})}{\beta N} \sum_{kk'\sigma\sigma'} \bar{c}_{k+q,\sigma} c_{k,\sigma} \bar{c}_{k'-q,\sigma'} c_{k',\sigma'}\right] \\ &= \int \mathcal{D}\phi \exp\left[-\sum_q \frac{\beta N}{2} \phi_q V^{-1}(\mathbf{q}) \phi_{-q} - i \sum_q \phi_q \sum_{k\sigma} \bar{c}_{k-q,\sigma} c_{k,\sigma}\right], \quad (\text{A6}) \end{aligned}$$

we introduce two auxiliary fields χ_q and ϕ_q which separately relate to the singlet pairing order and charge den-

sity wave order in the following way:

$$\langle \chi_q \rangle = \frac{|U|}{\beta N} \langle \sum_k c_{k\downarrow} c_{q-k\uparrow} \rangle, \quad (\text{A7})$$

$$\langle \phi_q \rangle = \frac{2iV(\mathbf{q})}{\beta N} \langle \sum_{k\sigma} \bar{c}_{k+q,\sigma} c_{k,\sigma} \rangle. \quad (\text{A8})$$

After integrating out the fermionic degrees of freedom $\bar{c}_{k\sigma}$ and $c_{k\sigma}$, the partition function becomes $\mathcal{Z} = \int \mathcal{D}(\bar{\chi}, \chi, \phi) e^{-S[\bar{\chi}, \chi, \phi]}$ where

$$S[\bar{\chi}, \chi, \phi] = \sum_q \left(\frac{\beta N}{|U|} |\chi_q|^2 + \frac{\beta N}{2} \phi_q V^{-1}(\mathbf{q}) \phi_{-q} \right) - \text{tr} \ln \hat{\mathcal{G}}^{-1}. \quad (\text{A9})$$

The matrix $\hat{\mathcal{G}}^{-1}$ have the following structure,

$$\hat{\mathcal{G}}^{-1} = \begin{pmatrix} \mathcal{G}_0^{p-1} + \Phi & \Lambda \\ \bar{\Lambda} & -\mathcal{G}_0^{p-1} + \tilde{\Phi} \end{pmatrix} \quad (\text{A10})$$

where matrices \mathcal{G}_0^{p-1} , Λ , $\bar{\Lambda}$, Φ , and $\tilde{\Phi}$ are given by $(\mathcal{G}_0^{p-1})_{kk'} = (i\omega_n - (\varepsilon(\mathbf{k}) - \mu)) \delta_{kk'}$, $\Lambda_{kk'} = \chi_{k+k'}$, $\bar{\Lambda}_{kk'} = \bar{\chi}_{k+k'}$, $\Phi_{kk'} = -i(\phi_{-k+k'})$, and $\tilde{\Phi}_{kk'} = i(\phi_{k-k'})$.

Before presenting a further analysis of the effective action $S[\bar{\chi}, \chi, \phi]$ in terms of the specific order parameter modes which we are interested in, one thing to be noted is that the zero mode of ϕ_q , i.e. $\phi_{(\mathbf{0},0)}$, corresponding to the particle density of the system, always has a non-vanishing contribution to the effective action $S[\bar{\chi}, \chi, \phi]$ independently of the system's parameters (interaction strength, temperature, etc). But on the other hand, we also note that the effect of $\phi_{(\mathbf{0},0)}$ is just to renormalize the chemical potential μ . Thus in the following analysis we simply neglect $\phi_{(\mathbf{0},0)}$ in $S[\bar{\chi}, \chi, \phi]$ by replacing the bare chemical potential μ with a renormalized one $\bar{\mu}$ which can be determined from the particle density of the system.

To simplify the notation, we further define

$$\hat{\mathcal{G}}_0^{-1} \equiv \begin{pmatrix} \mathcal{G}_0^{p-1} & 0 \\ 0 & -\mathcal{G}_0^{p-1} \end{pmatrix}, \quad (\text{A11})$$

$$\hat{\Phi} \equiv \begin{pmatrix} \Phi & 0 \\ 0 & \tilde{\Phi} \end{pmatrix}, \hat{\Lambda} \equiv \begin{pmatrix} 0 & \Lambda \\ \bar{\Lambda} & 0 \end{pmatrix}. \quad (\text{A12})$$

We note that

$$\text{tr} \ln \hat{\mathcal{G}}^{-1} = \text{tr} \ln \hat{\mathcal{G}}_0^{-1} + \text{tr} \ln [1 + \hat{\mathcal{G}}_0 \hat{\Lambda} + \hat{\mathcal{G}}_0 \hat{\Phi}], \quad (\text{A13})$$

where the first term just contributes a trivial constant. In the vicinity of the phase transition when both the order parameter fields ρ_q and Δ_q are small, we can expand the second term in (A13) in terms of $\hat{\mathcal{G}}_0 \hat{\Lambda}$ and $\hat{\mathcal{G}}_0 \hat{\Phi}$, i.e.,

$$\text{tr} \ln [1 + \hat{\mathcal{G}}_0 \hat{\Lambda} + \hat{\mathcal{G}}_0 \hat{\Phi}] = \sum_{n=1} \frac{(-1)^{n+1}}{n} \text{tr} (\hat{\mathcal{G}}_0 \hat{\Lambda} + \hat{\mathcal{G}}_0 \hat{\Phi})^n. \quad (\text{A14})$$

Odd order terms of either $\hat{\Lambda}$ or $\hat{\Phi}$ in the above expansion vanish since the effective action $S[\bar{\chi}, \chi, \phi]$ preserves the symmetry of the unordered phase. Since we are concerned with finite temperature phase transitions, we neglect the quantum fluctuations by treating χ_q and ϕ_q to be independent of Matsubara frequency, i.e., we focus on the zero Matsubara frequency component of χ_q and ϕ_q . Furthermore we assume that $\chi_{(\mathbf{0},0)}$, $\phi_{(\mathbf{Q},0)}$ and their conjugate dominate the effective interaction $S[\bar{\chi}, \chi, \phi]$, where $\mathbf{Q} = (\pi, \pi)$. From the above expansion formula (A14), the Ginzburg-Landau coefficients $\{A_\Delta, B_\Delta, A_\rho, B_\rho, C_{\Delta\rho}\}$ can be calculated explicitly.

In the following, we calculate the GL coefficient $C_{\Delta\rho}$ which we are most interested in. Expanding $S[\bar{\chi}, \chi, \phi]$ to the 4th order in $\chi_{(\mathbf{0},0)}$ and $\phi_{(\mathbf{Q},0)}$, the cross term between $\chi_{(\mathbf{0},0)}$ and $\phi_{(\mathbf{Q},0)}$ is given by

$$\begin{aligned} & \frac{1}{4} \left\{ 2\text{tr} \left[\left(\hat{\mathcal{G}}_0 \hat{\Lambda} \hat{\mathcal{G}}_0 \hat{\Phi} \right)^2 \right] + 4\text{tr} \left[\left(\hat{\mathcal{G}}_0 \hat{\Lambda} \right)^2 \left(\hat{\mathcal{G}}_0 \hat{\Phi} \right)^2 \right] \right\} \\ &= \sum_{\mathbf{k}, i\omega_n} \left[\frac{4}{(\xi^2(\mathbf{k}) + \omega_n^2)(i\omega_n - \xi(\mathbf{k}))(i\omega_n - \xi(\mathbf{k} + \mathbf{Q}))} \right. \\ & \quad \left. + \frac{2}{(\xi^2(\mathbf{k}) + \omega_n^2)(\xi^2(\mathbf{k} + \mathbf{Q}) + \omega_n^2)} \right] |\chi_{(\mathbf{0},0)}|^2 |\phi_{(\mathbf{Q},0)}|^2 \\ &= C_{\chi\phi} |\chi_{(\mathbf{0},0)}|^2 |\phi_{(\mathbf{Q},0)}|^2 \end{aligned} \quad (\text{A15})$$

where $\xi(\mathbf{k}) = \varepsilon(\mathbf{k}) - \bar{\mu}$. It accounts for the competition between singlet pairing and CDW order. From (A7) and (A8) we easily obtain $\langle \chi_{(\mathbf{0},0)} \rangle = |U|\Delta$ and $\langle \phi_q \rangle = 2iV(\mathbf{q})\rho_{\mathbf{Q}}$ which gives $C_{\Delta\rho} = C_{\chi\phi} 4V^2(\mathbf{Q})U^2$ after identifying the effective action $S[\bar{\chi}, \chi, \phi]$ with the Ginzburg-Landau free energy.

Now we calculate $C_{\chi\phi}$. The summation over Matsubara frequency can be performed explicitly:

$$\begin{aligned}
& \sum_{i\omega_n} \left[\frac{4}{(\xi^2(\mathbf{k}) + \omega_n^2)(i\omega_n - \xi(\mathbf{k}))(i\omega_n - \xi(\mathbf{k} + \mathbf{Q}))} + \frac{2}{(\xi^2(\mathbf{k}) + \omega_n^2)(\xi^2(\mathbf{k} + \mathbf{Q}) + \omega_n^2)} \right] \\
&= \left(\frac{-\beta}{2\pi i} \right) \oint dz \frac{1}{e^{\beta z} + 1} \left[\frac{4}{(z - \xi(\mathbf{k}))^2(z + \xi(\mathbf{k}))(z - \xi(\mathbf{k} + \mathbf{Q}))} + \frac{2}{(z^2 - \xi^2(\mathbf{k}))(z^2 - \xi^2(\mathbf{k} + \mathbf{Q}))} \right] \\
&= \beta \left[\frac{1}{\xi(\mathbf{k}) + \xi(\mathbf{k} + \mathbf{Q})} \left(\frac{4}{(1 + e^{\beta\xi(\mathbf{k} + \mathbf{Q}))}(\xi(\mathbf{k} + \mathbf{Q}) - \xi(\mathbf{k}))^2} - \frac{e^{\beta\xi(\mathbf{k})}}{(1 + e^{\beta\xi(\mathbf{k})})\xi^2(\mathbf{k})} \right) \right. \\
&\quad + \frac{\xi(\mathbf{k} + \mathbf{Q}) - 3\xi(\mathbf{k}) + e^{\beta\xi(\mathbf{k})}(\xi(\mathbf{k} + \mathbf{Q}) + \xi(\mathbf{k}))(-3 + 2\beta(\xi(\mathbf{k} + \mathbf{Q}) - \xi(\mathbf{k})))}{(1 + e^{\beta\xi(\mathbf{k})})^2\xi^2(\mathbf{k})(\xi(\mathbf{k} + \mathbf{Q}) - \xi(\mathbf{k}))^2} \\
&\quad \left. + \frac{1}{\xi^2(\mathbf{k}) - \xi^2(\mathbf{k} + \mathbf{Q})} \left(\frac{\tanh \frac{\xi(\mathbf{k} + \mathbf{Q})}{2}}{\xi(\mathbf{k} + \mathbf{Q})} - \frac{\tanh \frac{\xi(\mathbf{k})}{2}}{\xi(\mathbf{k})} \right) \right]. \tag{A16}
\end{aligned}$$

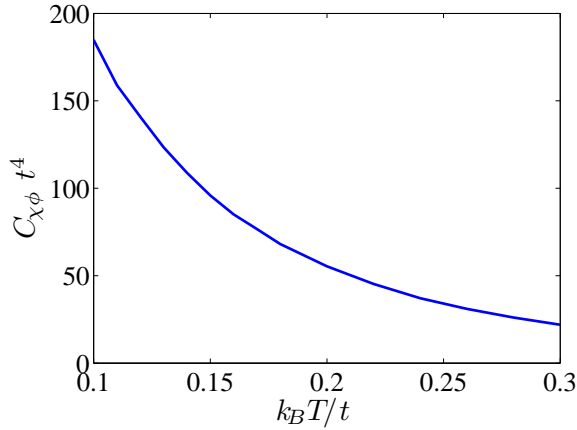


Figure 5: Temperature dependence of $C_{\chi\phi}$ at filling $\rho = 1.2$.

The remaining summation over momentum \mathbf{k} can be easily replaced by an integral over the density of states $\rho_{\text{DOS}}(\varepsilon) \equiv \sum_{\mathbf{k}} \delta(\varepsilon - \varepsilon(\mathbf{k}))$ and evaluated numerically. As we can see from Fig. 5, which shows the temperature dependence of $C_{\chi\phi}$ when $0.1 < k_B T/t < 0.3$ at filling $\rho = 1.2$, $C_{\chi\phi}$ is positive in this temperature region. Therefore, since the GL coefficient $C_{\Delta\rho}$ has the same sign as $C_{\chi\phi}$, we now clearly see that singlet pairing and CDW order indeed compete with each other in the parameter region under investigation.

-
- [1] D. Jaksch, C. Bruder, J. I. Cirac, C. W. Gardiner, and P. Zoller, *Phys. Rev. Lett.* **81**, 3108 (1998).
- [2] M. Greiner, O. Mandel, T. Esslinger, T.W. Hänsch, and I. Bloch, *Nature* **415**, 39 (2002).
- [3] I. Bloch, J. Dalibard, and W. Zwerger, *Rev. Mod. Phys.* **80**, 885 (2008).
- [4] W. Hofstetter, J. I. Cirac, P. Zoller, E. Demler and M. D. Lukin, *Phys. Rev. Lett.* **89**, 220407 (2002).
- [5] R. Jördens, N. Strohmaier, K. Günter, H. Moritz, and T. Esslinger, *Nature* **455**, 204 (2008).
- [6] S. Yi and L. You, *Phys. Rev. A* **61**, 041604 (2000).
- [7] S. Yi and L. You, *Phys. Rev. A* **63**, 053607 (2001).
- [8] K. Goral, K. Rzazewski, and T. Pfau, *Phys. Rev. A* **61**, 051601 (2000).
- [9] L. Santos, G. V. Shlyapnikov, P. Zoller, and M. Lewenstein, *Phys. Rev. Lett.* **85**, 1791 (2000).
- [10] S. Ronen, D. C. E. Bortolotti, and J. L. Bohn, *Phys. Rev. Lett.* **98**, 030406 (2007).
- [11] A. Griesmaier, J. Werner, S. Hensler, J. Stuhler, and T. Pfau, *Phys. Rev. Lett.* **94**, 160401 (2005).
- [12] J. Stuhler, A. Griesmaier, T. Koch, M. Fattori, T. Pfau, S. Giovanazzi, P. Pedri, and L. Santos, *Phys. Rev. Lett.* **95**, 150406 (2005).
- [13] A. Griesmaier, J. Stuhler, T. Koch, M. Fattori, T. Pfau, and S. Giovanazzi, *Phys. Rev. Lett.* **97**, 250402 (2006).
- [14] T. Lahaye, J. Metz, B. Fröhlich, T. Koch, M. Meister, A. Griesmaier, T. Pfau, H. Saito, Y. Kawaguchi, and M. Ueda, *Phys. Rev. Lett.* **101**, 080401 (2008).
- [15] K. Goral, L. Santos, and M. Lewenstein, *Phys. Rev. Lett.* **88**, 170406 (2002).
- [16] S. Yi, T. Li, and C. P. Sun, *Phys. Rev. Lett.* **98**, 260405 (2007).
- [17] B. Capogrosso-Sansone, C. Trefzger, M. Lewenstein, P. Zoller, and G. Pupillo, *Phys. Rev. Lett.* **104**, 125301 (2010).
- [18] L. Pollet, J. D. Picon, H. P. Büchler, and M. Troyer, *Phys. Rev. Lett.* **104**, 125302 (2010).
- [19] K. Góral, B.-G. Englert, and K. Rzazewski, *Phys. Rev. A* **63**, 033606 (2001).
- [20] M. A. Baranov, M. S. Marenko, Val. S. Rychkov, and G. V. Shlyapnikov, *Phys. Rev. A* **66**, 013606 (2002).
- [21] M. A. Baranov, Ł. Dobrek, and M. Lewenstein, *Phys. Rev. Lett.* **92**, 250403 (2004).
- [22] M. A. Baranov, K. Osterloh, and M. Lewenstein, *Phys.*

- Rev. Lett. **94**, 070404 (2005).
- [23] K. Osterloh, N. Barberán, and M. Lewenstein, Phys. Rev. Lett. **99**, 160403 (2007).
- [24] K.-K. Ni, S. Ospelkaus, M. H. G. de Miranda, A. Pe'er, B. Neyenhuis, J. J. Zirbel, S. Kotochigova, P. S. Julienne, D. S. Jin, and J. Ye, Science **322**, 231 (2008).
- [25] L. He, J. N. Zhang, Y. Zhang, and S. Yi, Phys. Rev. A **77**, 031605(R) (2008).
- [26] T. Miyakawa, T. Sogo, and H. Pu, Phys. Rev. A **77**, 061603(R) (2008).
- [27] G. M. Bruun and E. Taylor, Phys. Rev. Lett. **101**, 245301 (2008).
- [28] T. Sogo, L. He, T. Miyakawa, S. Yi, H. Lu, and H. Pu, New J. Phys. **11**, 055017 (2009).
- [29] J.-N. Zhang and S. Yi, Phys. Rev. A **80**, 053614 (2009).
- [30] K. Sun, C. -J. Wu, and S. Das Sarma, Phys. Rev. B **82**, 075105 (2010).
- [31] Y. Yamaguchi, T. Sogo, T. Ito, and T. Miyakawa, Phys. Rev. A **82**, 013643 (2010).
- [32] C. Zhao, L. Jiang, X.-X. Liu, W. M. Liu, X.-B. Zou, and H. Pu, Phys. Rev. A **81**, 063642 (2010).
- [33] A. R. P. Lima and A. Pelster, Phys. Rev. A **81**, 063629 (2010).
- [34] Y. Endo, T. Miyakawa, and T. Nikuni, Phys. Rev. A **81**, 063624 (2010).
- [35] J.-N. Zhang and S. Yi, Phys. Rev. A **81**, 033617 (2010).
- [36] A. R. P. Lima and A. Pelster, Phys. Rev. A **81**, 021606 (2010).
- [37] C.-K. Chan, C.-J. Wu, W.-C. Lee, and S. Das Sarma, Phys. Rev. A **81**, 023602 (2010).
- [38] S. Ronen and J. L. Bohn, Phys. Rev. A **81**, 033601 (2010).
- [39] C.-H. Lin, Y.-T. Hsu, H. Lee, and D.-W. Wang, Phys. Rev. A **81**, 031601 (2010).
- [40] C.-W. Lin, E. Zhao, and W. V. Liu, Phys. Rev. B **81**, 045115 (2010).
- [41] C.-J. Wu and J. E. Hirsch, Phys. Rev. B **81**, 020508 (2010).
- [42] T. Shi, J.-N. Zhang, C.-P. Sun, and S. Yi, Phys. Rev. A **82**, 033623 (2010).
- [43] K. Mielsonson and J. K. Freericks, Phys. Rev. A **83**, 043609 (2011).
- [44] K.-K. Ni, S. Ospelkaus, D. Wang, G. Quémener, B. Neyenhuis, M. H. G. de Miranda, J. L. Bohn, J. Ye, and D. S. Jin, Nature **464**, 1324 (2010).
- [45] M. Snoek, I. Titvinidze, C. Toke, K. Byczuk, and W. Hofstetter, New J. Phys. **10**, 093008 (2008).
- [46] R. W. Helmes, T. A. Costi, and A. Rosch, Phys. Rev. Lett. **100**, 056403 (2008).
- [47] A. Georges, G. Kotliar, W. Krauth, and M. J. Rozenberg, Rev. Mod. Phys. **68**, 13 (1996).
- [48] G. Kotliar, S. Y. Savrasov, G. Pálsson, and G. Biroli, Phys. Rev. Lett. **87**, 186401 (2001).
- [49] E. Müller-Hartmann, Z. Phys. B **74**, 507 (1989).
- [50] M. Caffarel and W. Krauth, Phys. Rev. Lett. **72**, 1545 (1994).
- [51] Q.-M. Si, M. J. Rozenberg, G. Kotliar, and A. E. Ruckenstein, Phys. Rev. Lett. **72**, 2761 (1994).
- [52] P. Bak and R. Bruinsma, Phys. Rev. Lett. **49**, 249 (1982).
- [53] T. Gericke, P. Würtz, D. Reitz, T. Langen, and H. Ott, Nature Phys. **4**, 949 (2008).
- [54] W. S. Bakr, J. I. Gillen, A. Peng, S. Fölling, and M. Greiner, Nature **462**, 74 (2009).
- [55] W. S. Bakr, A. Peng, M. E. Tai, R. Ma, J. Simon, J. I. Gillen, S. Fölling, L. Pollet, and M. Greiner, Science **329**, 5991 (2010).
- [56] J. F. Sherson, C. Weitenberg, M. Endres, M. Cheneau, I. Bloch, S. Kuhr, Nature **467**, 68 (2010).
- [57] S. Robaszkiewicz, R. Micnas, and K. A. Chao, Phys. Rev. B **24**, 1579 (1981).
- [58] M. Popp, J.-J. Garcia-Ripoll, K. G. Vollbrecht, and J. I. Cirac, Phys. Rev. A **74**, 013622 (2006).
- [59] T. Ho, Q. Zhou, Natl. Acad. Sci. U.S.A. **106**, 6916 (2009).
- [60] J. Catani, G. Barontini, G. Lamporesi, F. Rabatti, G. Thalhammer, F. Minardi, S. Stringari, and M. Inguscio, Phys. Rev. Lett. **103**, 140401 (2009).
- [61] D. M. Weld, P. Medley, H. Miyake, D. Hucul, D. E. Pritchard, and W. Ketterle, Phys. Rev. Lett. **103**, 245301 (2009).
- [62] P. Medley, D. M. Weld, H. Miyake, D. E. Pritchard, and W. Ketterle, arXiv:1006.4674.